Indian Journal of Pure & Applied Physics
Vol. 52, December 2014, pp. 821-828

Investigation on the properties of L-serine doped zinc tris (thiourea) sulphate crystal for NLO application

F Helen[a] & G Kanchana[a]*

[a]PG and Research Department of Physics, Government Arts College, Coimbatore 641 018, Tamilnadu, India

*E-mail: kanchanagopinath@gmail.com

Received 9 September 2013; revised 27 August 2014; accepted 3 November 2014

Single crystals of L-serine doped zinc tris (thiourea) sulphate (LSZTS) were grown by the slow evaporation solution growth technique (SEST) at room temperature. The LSZTS crystals were subjected to powder XRD to confirm the crystalline nature and purity of the crystal. The lattice parameters of LSZTS were obtained from single crystal X-ray diffraction analysis. Fourier transform infrared (FTIR) and Raman (FT-Raman) spectroscopic studies revealed the functional groups present in the doped crystal. Ultraviolet visible (UV-Vis) transmittance spectrum showed that the lower cutoff wavelength of LSZTS was 325 nm. Theoretical calculations were carried out to determine the linear optical constants. Photoluminescence (PL) spectrum of the LSZTS showed blue emission. The thermo gravimetry (TG) and differential scanning calorimetry (DSC) analyses revealed that LSZTS crystal was stable up to 231.9πC. Microhardness study was carried out to assess the mechanical stability of the doped crystal. The work hardening coefficient of LSZTS was estimated. Kurtz Perry powder test was carried out to study the effect of L-serine on the NLO properties of ZTS. The second harmonic generation (SHG) efficiency of LSZTS was found to be enhanced in the presence of a high concentration of dopant.

Keywords: Growth from solutions, X-ray diffraction, Microhardness, Optical properties, NLO material

1 Introduction

In the past two decades, nonlinear optical crystals have attracted the attention of scientists and technologists due to their potential applications in the area of photonics including optical information, processing high energy laser, colour display and frequency conversion. In recent years, efforts have been made to develop UV lasers for photonics, optoelectronics, infrared and medical applications[1-3].

The nonlinear optical property of amino acid crystals has contributed to the tremendous progress that has been made in the development of coherent UV sources. Organic crystals possess special properties of large optical nonlinearity and low cutoff wavelength in the UV-region and consequently the organic NLO crystals are used in optical devices. However, organic crystals have certain limitations such as poor mechanical and thermal stability. To overcome these problems, a combination of organic and inorganic hybrid compounds has been developed. These compounds constitute a new class of materials called semi-organic materials that are characterized by large optical nonlinearity, higher mechanical strength and chemical stability.

Many natural amino acids individually exhibit the NLO properties, because they have chiral symmetry and often crystallise in non-centro symmetric space groups. L-serine is an organic compound under the amino acid category. It is one of the naturally occurring proteinogenic amino acids. L-serine exists in zwitter ionic form and the molecule can combine with anionic, cationic and overall neutral constituents[4].

ZTS is a metal organic crystal with a high laser damage threshold and a wide range of transparency. ZTS crystal belongs to the orthorhombic crystal system with the space group[5-8] $Pca2_1$. In the present paper, the effect of L-serine on ZTS crystals has been studied. It has been shown that some of the dopants enhance the optical, mechanical, electrical properties and chemical stability. A series of metal ion and amino acid doped ZTS crystals with moderate mechanical and thermal stability have been reported[8-11].

The optically transparent, good quality L-serine doped ZTS (LSZTS) crystals have been grown and the influence of L-serine on the properties of pure ZTS has been described. The grown crystals were subjected to various characterization techniques. The effect of two different concentrations of L-serine on the SHG efficiency has been investigated.

2 Experimental Details

2.1 Synthesis and crystal growth

Thiourea and zinc sulphate heptahydrate (AR grade) were taken in the ratio of 3:1 and dissolved in deionised water. The solution was stirred using a magnetic stirrer and ZTS salt was synthesized. Recrystallization was carried out to improve the purity of the synthesized salt. A saturated solution was prepared using the recrystallized salt and de-ionized water at room temperature with continuous stirring. The solution was then filtered using Whatmann filter paper and covered with a perforated sheet. It was left undisturbed for slow evaporation. For the growth of L-serine doped ZTS crystals, 0.1 M and 0.5 M of L-serine were added to the saturated solution of ZTS and stirred continuously to ensure homogeneous concentration. The initial *p*H of the solution was kept at 3.5. The solution was filtered and kept undisturbed for slow evaporation.

Pure and L-serine doped ZTS single crystals with good quality and well defined morphology were harvested after 15 days. The photographs of the pure ZTS, L-serine doped ZTS crystals are shown in Fig. 1.

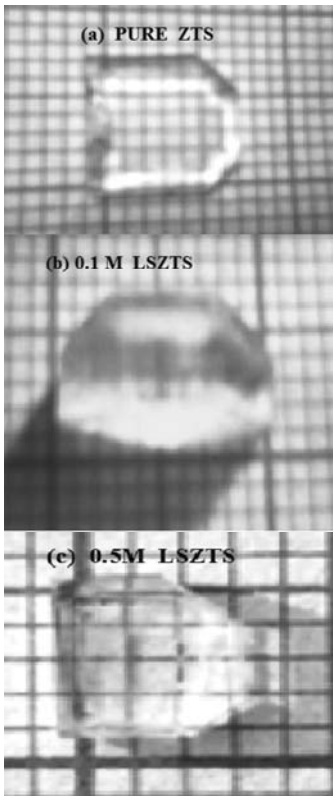

Fig. 1 — As grown crystals of (a) pure ZTS (b) 0.1 M LSZTS (c) 0.5 M LSZTS

2.2 Characterization studies

The SHG measurements were carried out on the powdered crystals using the Kurtz Perry powder technique. Since 0.5 M LSZTS was found to have the highest SHG efficiency, further characterization studies were carried out for 0.5 M LSZTS only. The powder XRD analysis was carried out by employing the Rigaku Ultima III X-ray diffractometer to study the crystalline nature of the grown crystal. The unit cell parameters of pure and doped crystals were obtained from single crystal XRD studies using the Enraf Nonius CAD 4 diffractometer. FTIR spectrum of the sample was recorded between 4000 cm^{-1} and 400 cm^{-1} by the KBr Pellet technique using the Perkin Elmer spectrometer. The FT-Raman spectrum of the grown crystal was recorded using the BRUKER: RFS 27 FT-Raman spectrometer. The optical properties of LSZTS were studied in the range 200-1100 nm using the Perkin Elmer Lamda 35 UV-Vis-NIR spectrometer. Thermal analyses were carried out by employing NETZSCHSTA 409 in the temperature range 50°-750°C at the heating rate of 10°C/min in nitrogen atmosphere. The Vicker's microhardness test was carried out to estimate the mechanical strength of the crystals. Photoluminescence emission spectrum was recorded to observe the emission band.

3 Results and Discussion

3.1 *SHG test*

The effect of L-serine of different concentrations on the NLO property of the ZTS crystal was studied by the Kurtz and Perry powder technique[12]. The powder sample of pure and L-serine doped ZTS crystal were illuminated using the fundamental beam of 1064 nm from Q-switched Nd: YAG laser, which generated an input power of 4.2 mJ/pulse. The input laser beam was passed through an IR reflector and then directed on the microcrystalline powdered sample packed in a capillary tube. The output power for pure ZTS, 0.1 M LSZTS and 0.5 M LSZTS was 7, 6.8 and 8 mV, respectively for the same input power.

Low doping (0.1 M LSZTS) had no significant influence on NLO properties of ZTS crystals. The SHG efficiency of 0.5 M LSZTS was 1.14 times that of pure ZTS. It was observed that the SHG efficiency was enhanced in the case of the heavily doped ZTS crystal. Hence, further characterization studies were carried out for 0.5M LSZTS.

It has been suggested that when ZTS reacts with L-serine, the optically active amino group may get

added in the structure of ZTS. This increases its non-centro symmetry and consequently increases the SHG efficiency. The efficiency of the frequency conversion will vary with the particle size and the orientation of the crystallites in the capillary tube. Hence, higher efficiency may be expected to be achieved with single crystals by optimizing the phase matching[13].

3.2 X-ray diffraction analysis

The fine powder of 0.5 M of L-serine doped ZTS was subjected to powder X-ray diffraction analysis. The powder sample was scanned in steps of 0.02° for a 2θ range of 10° to 60°. The sharp and well defined Bragg's peaks at specified 2θ angles confirm the crystalline nature and purity of the crystal[14]. All the peaks are indexed and the recorded pattern is shown in Fig. 2.

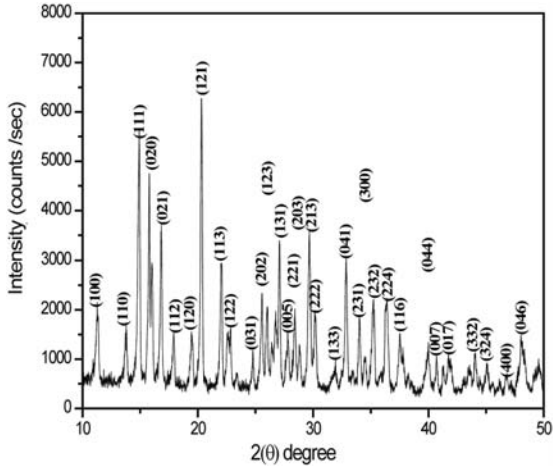

Fig. 2 — Powder XRD of 0.5 M LSZTS

The lattice parameters of pure and L-serine doped ZTS crystals were determined by single crystal XRD analysis. The structure was confirmed to be orthorhombic with the space group $Pca2_1$. The lattice parameters of pure and LSZTS are listed in Table 1. The observed values are found to be in good agreement with the reported data[7] of pure ZTS.

3.3 FTIR and FT-Raman analyses

Spectroscopic studies (FTIR and FT-RAMAN) have been used to elucidate the functional groups of the 0.5 M LSZTS crystal. The FTIR and FT-Raman spectra are shown in Figs 3 and 4, respectively. The functional groups were identified by the FTIR studies and confirmed by the FT-Raman studies.

The bands in the region from 3415 cm^{-1} to 2594 cm^{-1} are assigned to NH_2 symmetric and asymmetric

Table 1 — Single crystal XRD of pure ZTS and LSZTS

Cell parameter	Pure ZTS [Ref.7]	Pure ZTS (present study)	0.1 M LSZTS	0.5 M LSZTS
a(Å)	7.792	7.765	7.774	7.782
b(Å)	11.111	11.136	11.133	11.145
c(Å)	15.478	15.510	15.500	15.493
α =β =γ	90°	90°	90°	90°
V (Å)^3	1340.1	V=1341.2	1341.4	1343.8

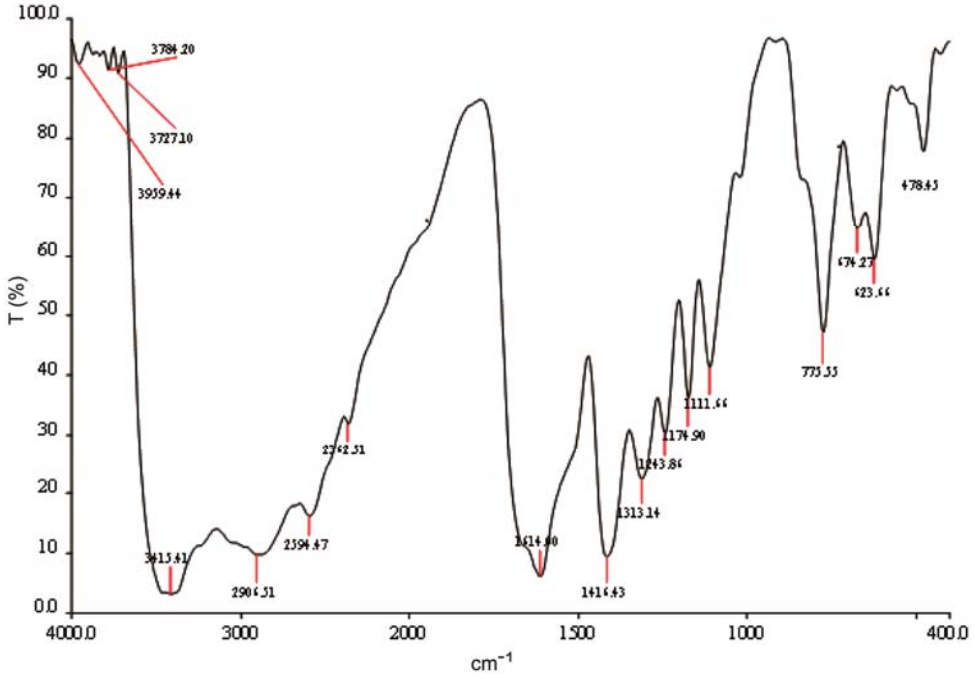

Fig. 3 — FTIR spectrum

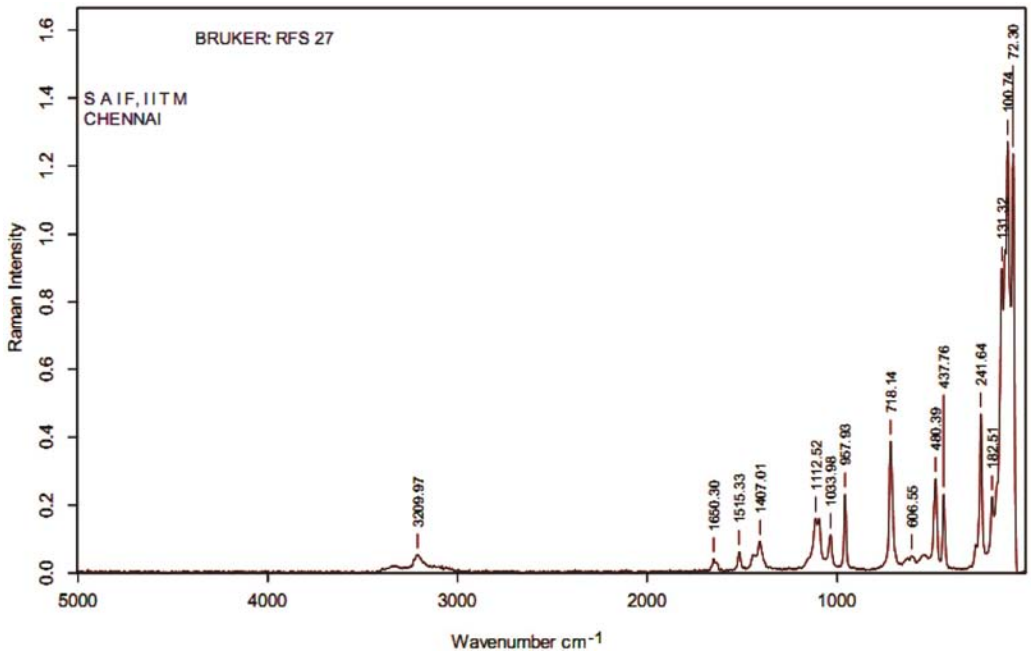

Fig. 4 — FT-Raman spectrum

stretching vibrations. The peaks at 1614 cm^{-1} in IR, 1650 cm^{-1} in Raman correspond to NH_2 bending. The peaks at 1515 cm^{-1} and 1033 cm^{-1} in Raman spectra are due to S=C-N stretching vibrations. C=S asymmetric stretching vibration gives its peak at 1 416 cm^{-1} in IR and 1407 cm^{-1} in Raman. The peaks at 1111 cm^{-1} in FTIR and 1112 cm^{-1} in FT-Raman are assigned to symmetric stretching vibrations of sulphate ion. C-N symmetric stretching vibration produces its peak at 775 cm^{-1} in FTIR and 718 cm^{-1} in FT-Raman. The presence of sulphate ion is evident from the peaks at 957 cm^{-1} and 437 cm^{-1} in Raman spectra. The peaks at 623 cm^{-1} in IR and 606 cm^{-1} in Raman reveal the presence of sulphate ion. An increase in the number of NH_2 stretching vibrations in IR and Raman spectra establishes the presence of the amino group of L-serine in the lattice of LSZTS crystal[5].

3.4 UV-vis-NIR spectral analysis

The study of optical absorption of a material is important for NLO applications. In order to find the suitability of the material for optical application, the UV-Vis absorption and transmission spectra were recorded in the range 200-1100 nm. A single crystal of 0.5 M LSZTS with a thickness of 1.5 mm was used for this purpose. The transmittance spectrum is shown in Fig. 5. The percentage of transmittance is about

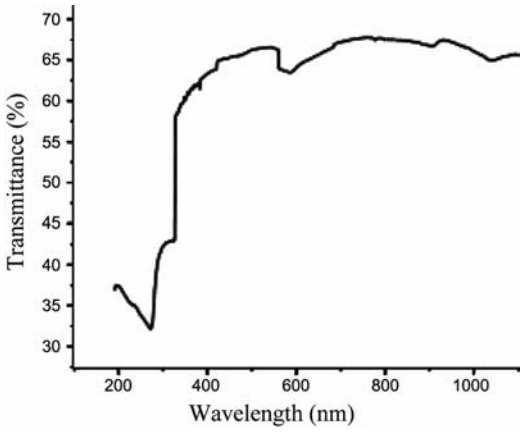

Fig. 5 — UV-VIS transmission spectrum

67% in the LSZTS crystal. The lower cut off occurs at 325 nm in the LSZTS crystal. The crystal is found to be transparent in the visible and near IR region, an essential parameter required for frequency doubling process[15].

The optical absorption coefficient α was calculated using the following relation:

$$\alpha = \frac{2.303 \log\left(\frac{1}{T}\right)}{d} \qquad \ldots(1)$$

where T is the transmittance and d is the thickness of the crystal.

The energy dependence of absorption coefficient suggests the occurrence of direct band gap and hence it obeys the relation for high photon energy.

$$(\alpha hv)^2 = A(hv - E_g) \quad \ldots(2)$$

where E_g is optical band gap and A is a constant. The variation of (hv) versus $(\alpha hv)^2$ is shown in Fig. 6 and E_g value is evaluated by extrapolation of the linear portion near the onset of absorption edge to the energy axis. The optical band gap is found to be 4.1 eV.

The various other optical constants were calculated using the following theoretical formulae. The extinction coefficient (K) is obtained in terms of the absorption coefficient:

$$K = \frac{\lambda\alpha}{4\pi} \quad \ldots(3)$$

where λ is the wavelength. The reflectance (R) in terms of absorption coefficient is derived from the relation:

$$R = \frac{1 \pm (1 - \exp(-\alpha d) + \exp(\alpha d)^{1/2}}{1 + \exp(-\alpha d)} \quad \ldots(4)$$

and the linear refractive index (n) is given by:

$$n = \frac{-(R + 1 + \pm(-3R^2 + 10R - 3)^{1/2}}{2(R-1)} \quad \ldots(5)$$

From the recorded absorption spectra, the linear optical constants of LSZTS were calculated. The variation of optical constants K and R as a function of photon energy are shown in Figs 7 and 8. The extinction coefficient shows exponential decay as the photon energy increases. Refractive index being the measure of percentage of intensity of light reflected, the reflectance increases with photon energy.

From Figs 7 and 8, it is clear that the extinction coefficient and the reflectance depend upon the absorption coefficient. The high transmission, low absorbance, low reflectance makes the material a prominent one for anti-reflection coating in solar thermal devices and nonlinear optical applications[16]. It is importantly noticed that the crystal has positive refractive index (n = 1.3 at 4 eV) with respect to photon energy and this indicates the focusing nature of the crystal[17].

The high transmittance percentage together with the wide transparency window is sufficient for the second harmonic generation. Hence, this material may

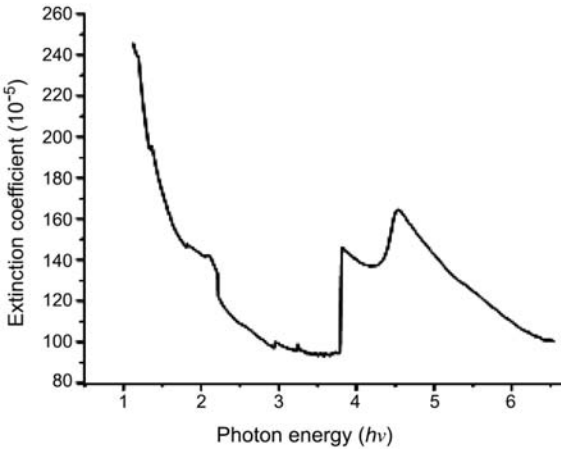

Fig. 7 — Photon energy versus extinction coefficient

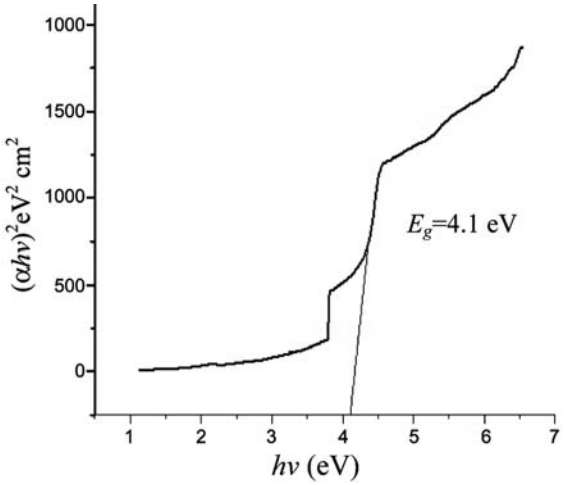

Fig. 6 — Photon energy versus optical band gap

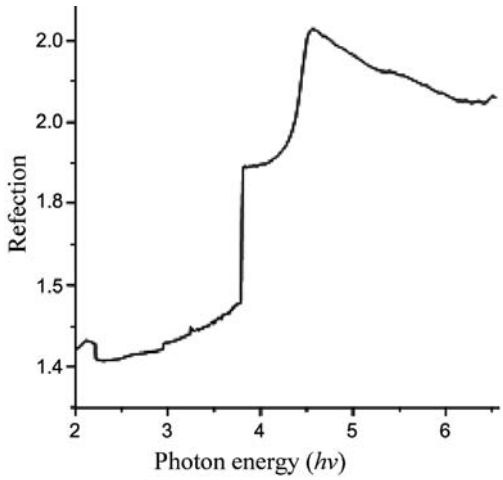

Fig. 8 — Photon energy versus reflectance

prove useful in the fabrication of optoelectronic and nonlinear optical devices.

3.5 Thermal analysis

The TGA and DSC thermograms of 0.5 M LSZTS are shown in Fig. 9. There occurs no weight loss for up to 231.9°C in the TG curve. This indicates that there is no inclusion of water in the crystal lattice. DSC thermogram indicates the absence of any exotherm or endotherm up to 231.9°C, indicating no solvent inclusion in the crystal lattice which is also supported by TGA data.

A major weight loss observed at 231.9°C in the TG curve is assigned to the decomposition of the title compound. A sharp endothermic peak at 231.9°C in the DSC curve that corresponds to the weight loss in the TG curve may be due to the decomposition of the crystal. It is observed that there is no phase transition observed in the crystal below 231.9°C. Thus LSZTS is stable for up to 231.9°C.

Hence, the material can be used for NLO application below its decomposition temperature[18]. The endotherms which appear above this temperature are due to the phase transitions of LSZTS. The thermal stability of L-serine doped ZTS crystal is higher than L-alanine doped ZTS crystal[9] and is marginally low when compared to glycine doped ZTS crystal[10].

3.6 Microhardness

Microhardness is the measure of strength of the material and is an important mechanical property of the optical materials in the fabrication of devices. Physically hardness is the resistance offered by the material to localized plastic deformation (movement of dislocations) caused by scratching or indentation[19]. Vickers microhardness studies were carried out on 0.5 M LSZTS crystal by applying load of different magnitudes. The indentation time was fixed constant for each trial. Repeated trials were performed to ascertain the correctness of the observed results. The Vickers microhardness number H_v was calculated using the relation:

$$H_v = 1.8544\left(\frac{P}{d^2}\right) \text{kg/mm}^2 \qquad \ldots(6)$$

where P is the load in kg and d is the diagonal length of indentation impression in mm. The plot of load(P) versus Vickers hardness number (H_v) is shown in Fig. 10. It is observed that the hardness number increases with increasing load indicating the reverse indentation size effect[20] [RISE]. The increase in hardness with the load could be attributed to the heaping up of materials at the edges of impression made by the diamond pyramid[21]. The hardness value of 0.5 M LSZTS crystal is found to be 65.85 kg/mm^2 for a load of 100 g which confirms the good mechanical stability of the crystal.

The relation between load and size of the indentation is given by Meyer's law:

$$P = K_1 d^n \qquad \ldots(7)$$

where K_1 is a constant for a given material and n is the work hardening coefficient (Meyer index).

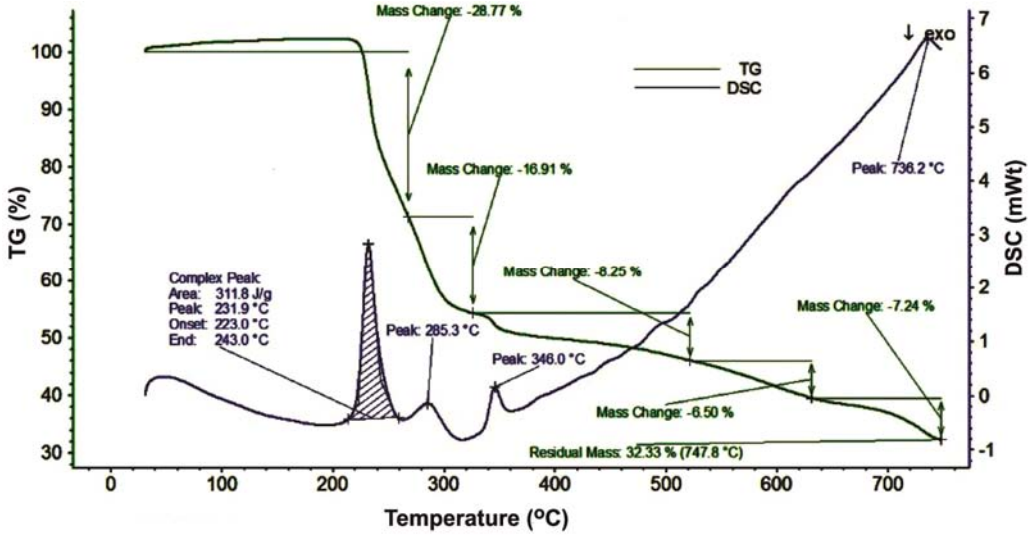

Fig. 9 — TGA/DSC thermograms

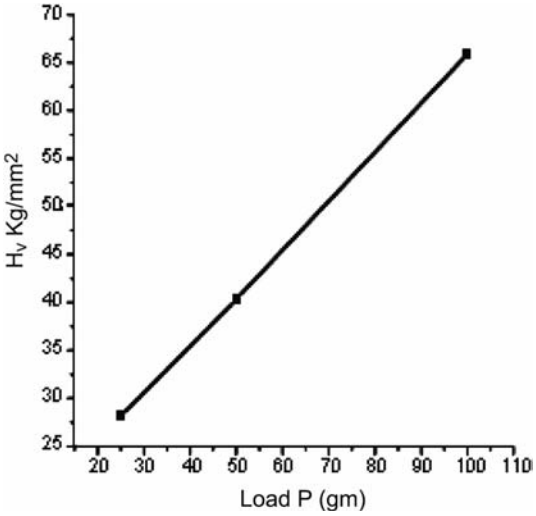

Fig. 10 — Plot of load versus hardness number

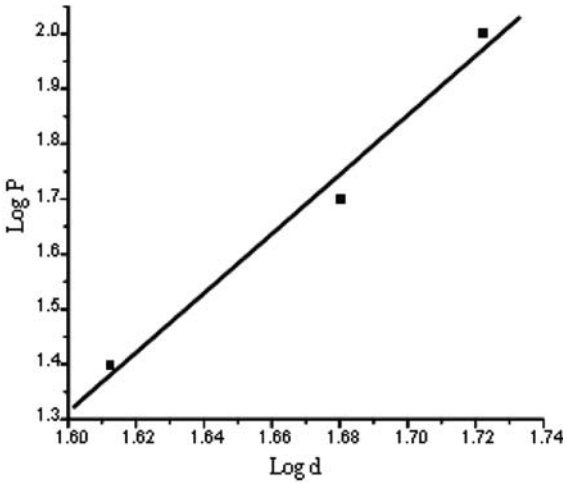

Fig. 11 — Plot of log d versus log P

Figure 11 shows the least square fit plot of log(d) versus log(P). The slope of the straight line gives the work hardening coefficient (n). According to Onitsch, n should lie between 1 and 1.6 for hard materials and should be greater than 1.6 for soft materials[22]. Since n is 5.39 for 0.5 M LSZTS, it is concluded that the LSZTS crystal is a soft material.

3.7 Photoluminescence study

In photoluminescence (PL) technique, the spectrum emitted by the radioactive recombination of photo generated minority carriers is used to measure the band gap energy. However, a large amount of impurities induces a large free carrier density in the bands. Consequently, a different carrier interaction causes remarkable modification of the line shape and

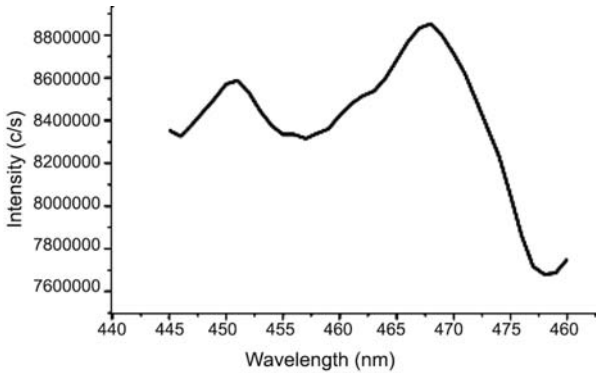

Fig. 12 — PL spectrum of 0.5 M LSZTS

spectral energy of PL spectra[23]. 0.5M LSZTS sample was excited at 250 nm. The emission spectrum is shown in Fig. 12. The emission peaks are observed at 450 nm and 468 nm. These are due to the molecular donor carboxyl (COO^-) group, acceptor amino (NH_2^+) group that can enhance the mobility of electrons. The high intensity peak at 468 nm indicates that 0.5M LSZTS crystal has blue fluorescence emission.

4 Conclusions

The single crystals of pure and L-serine doped ZTS were successfully grown using the slow evaporation solution growth technique. The effects of L-serine on the properties of ZTS have been studied. The observed values of lattice parameters of the doped crystals are in good agreement with the reported data of pure ZTS. The FTIR and FT-Raman studies confirm the presence of various functional groups. Further, the increase in NH_2 stretching vibrations in FTIR and Raman spectra establishes the presence of amino group of L-serine in the lattice of ZTS crystal.

The TGA and DSC thermograms prove that the 0.5M LSZTS can be exploited for any suitable application up to 231.9°C. The microhardness test confirms the good mechanical stability of L-serine doped ZTS crystal. The percentage of transmittance of 0.5 M LSZTS crystal is about 67%. The lower cut off wavelength is around 325 nm. The wide range of transparency of LSZTS is an added advantage in the field of optoelectronic application. The high transmission, low absorbance, low reflectance of LSZTS in the UV and visible region make the material a prominent one for anti-reflection coating in solar thermal devices. The positive refractive index indicates the focusing nature of the crystal. The photoluminescence spectrum shows blue fluorescence

emission. The Kurtz Perry powder test shows that the presence of high concentration of L-serine enhances the SHG efficiency of ZTS crystal. The good thermal, mechanical and optical properties together with better SHG efficiency make L-serine doped ZTS, a potential material for NLO and laser applications.

Acknowledgement

The authors would like to acknowledge the support extended to this research by SAIF, Indian Institute of Technology, Chennai, Indian Institute of Science, Bangalore and St Joseph's College, Trichy.

References

1 Marcy H O, Warren L F, Webb M S, *et al.*, *Appl Opt,* 31 (1992) 5051.
2 Santhakumari R, Ramamurthi K, Ramesh Babu R, *et al.*, *Specctrochim Acta A,* 82 (2011) 102.
3 Meredith G R, *Nonlinear optical properties of organic and polymer material* in ACS symposium series, edited by D J Williams, (American Chemical Society, Washington DC), 1982, p. 27.
4 Parthasarathy M, Ananatharaja M & Gopalakrishnan R, *J Cryst Growth,* 340 (2012) 118.
5 Sweta Moitra & Tanusree Kar, *Opt Mater,* 30 (2007) 508.
6 Venkataraman V, Dhanaraj G, WadhawanV K, *et al.*, *J Cryst Growth,* 154 (1995) 92.
7 Ushasree P M, Jayavel R, Subramanian C & Ramasamy P, *J Cryst Growth*, 197 (1999) 216.
8 Gopinath S, Palanivel R & Rajasekaran R, *Int J Pure Appl Sci Technol,* 1(2) (2010) 104.
9 Dhumane N R, Hussaine S S, Kunal Datta *et al.*, *Rec Res Sci Tech*, 2 (2010) 30.
10 Dhumane N R, Hussaine S S, Dongre V & Mahendra D Shirsat *Opt Mater*, 31 (2008) 328.
11 Muthu K & Meenakshisundaram S P, *J Phys Chem Solids,* 73 (2012) 1146.
12 Kurtz S K & Perry T T*, J Appl Phys,* 39 (1968) 3798.
13 Balasubramanian D, Murugakoothan P & Jayavel R, *J Cryst Growth,* 312 (2010) 1855.
14 Delci Z, Shyamala D, Karuna S, et al, *Indian J Pure & Appl Phys*, 51 (2013) 426.
15 Rao C N R, Ultraviolet *and Visible Spectroscopy of organic compounds* (Prentice Hall Pvt Ltd, New Delhi) 1984, 60.
16 Santhakumari R & Ramamurthi K, *Spectrochim Acta A,* 78 (2011) 653.
17 Peramaiyan G, Pandi P, Sornamurthi B M, *et al, Spectrochim Acta A*, 95 (2012) 310.
18 Shyamala D, Rajendran V, Natarajan R K & Moorthy Babu S, *Cryst Growth Des,* 7 (2007) 1695.
19 Saravanan R R, Seshadri S, Murugan M & Manivannan V, *Indian J Pure & Appl Phys*, 51 (2013) 254.
20 Sangwal K, Mater *Chem Phys*, 63 (2000) 145.
21 Ravishankar M N, Ahlam M A, Chandramani R & Gnana Prakash A P, *Indian J Pure & Appl Phys*, 51 (2013) 55.
22 Onitsch E M, *Mikroskopie,* 95 (1950) 12.
23 Madeswaran P, Thirumalairajan P & Chandrasekaran J, *Optik,* 121 (2010) 1620.